Numerical study of optimal trajectories with singular arcs for space launcher problems

Pierre Martinon, Frédéric J. Bonnans, Julien Laurent-Varin, Emmanuel Trélat

INSTITUT NATIONAL DE RECHERCHE EN INFORMATIQUE ET EN AUTOMATIQUE

Numerical study of optimal trajectories with singular arcs for space launcher problems

Pierre Martinon — Frédéric Bonnans — Julien Laurent-Varin — Emmanuel Trélat

N° ????

Fevrier 2008

Thème NUM

ISSN 0249-6399 ISRN INRIA/RR--????--FR+ENG

INSTITUT NATIONAL
DE RECHERCHE
EN INFORMATIQUE
ET EN AUTOMATIQUE

INRIA

centre de recherche
SACLAY - ÎLE-DE-FRANCE

Numerical study of optimal trajectories with singular arcs for space launcher problems

Pierre Martinon* , Frédéric Bonnans* , Julien Laurent-Varin† , Emmanuel Trélat‡ *

Thème NUM — Systèmes numériques
Équipes-Projets COMMANDS

Rapport de recherche n° ???? — Fevrier 2008 — 23 pages

Abstract: The subject of this paper is the study of singular arcs (i.e. with a non maximal thrust) for a space launcher problem. We consider a flight to the GTO orbit for a heavy multi-stage launcher (Ariane 5 class), and use a realistic physical model for the drag force and rocket thrust. As a preliminary result, we first solve the complete flight with stage separations, at full thrust. Then we focus on the first atmospheric climbing phase, to investigate the possible existence of optimal trajectories with singular arcs. We primarily use an indirect shooting method (based on Pontryagin's Minimum Principle), coupled to a continuation (homotopy) approach. Some additional experiments are made with a basic direct method, and confirm the solutions obtained by the shooting. We study two slightly different launcher models, and observe that modifying parameters such as the aerodynamic reference area and specific impulsion can indeed lead to optimal trajectories with either full thrust or singular arcs.

Key-words: optimal control, launcher problem, singular arcs, indirect shooting, continuation

* INRIA-Saclay and CMAP UMR CNRS 7641, Ecole Polytechnique, 91128 Palaiseau
† CNES, Direction des Lanceurs, Rond-point de l'Espace, Evry
‡ Université d'Orléans, Math., Lab. MAPMO, UMR CNRS 6628

Centre de recherche INRIA Saclay – Île-de-France
Parc Orsay Université
4, rue Jacques Monod, 91893 ORSAY Cedex
Téléphone : +33 1 72 92 59 00

Etude numérique de trajectoires optimales avec arcs singuliers pour un problème de lanceur spatial

Résumé : The subject of this paper is the study of singular arcs (i.e. with a non maximal thrust) for a space launcher problem. We consider a flight to the GTO orbit for a heavy multi-stage launcher (Ariane 5 class), and use a realistic physical model for the drag force and rocket thrust. As a preliminary result, we first solve the complete flight with stage separations, at full thrust. Then we focus on the first atmospheric climbing phase, to investigate the possible existence of optimal trajectories with singular arcs. We primarily use an indirect shooting method (based on Pontryagin's Minimum Principle), coupled to a continuation (homotopy) approach. Some additional experiments are made with a basic direct method, and confirm the solutions obtained by the shooting. We study two slightly different launcher models, and observe that modifying parameters such as the aerodynamic reference area and specific impulsion can indeed lead to optimal trajectories with either full thrust or singular arcs

Mots-clés : controle optimal, lanceur, arcs singuliers, methode de tir, continuation

Introduction

In this paper we investigate the possible occurence of singular arcs in the case of the European Ariane 5 space launcher, when maximizing the payload. Trajectory optimization for space launchers is a classical problem in optimal control, see for instance Pesch [13], Betts [2] for an overview of popular algorithms. By singular arc is meant an extremal arc along which the thrust is neither maximal nor equal to zero. For ascent problems with atmosphere a naive strategy is to have a maximal thrust as long as possible during the propulsion phase. However, full thrust may conduct to large values of speed that lead to important energy losses due to the drag forces. Extensive numerical experiments show that singular arcs may indeed occur in some cases. A simple model problem is the Goddard problem [7, 17], that consists in maximizing the final altitude of a rocket with vertical trajectory. For such problems, the second time derivative of the switching function (the latter is the partial derivative of the Hamiltonian w.r.t. the control) is an affine function function of the control, and for the models used in the literature, the coefficient of the control is nonzero. Equating this affine function to zero allows to express the control as a function of state and costate (the singular control law). In addition, since these models are three dimensional, it happens that the singular control law can be expressed as a function of the state only. A variant of the Goddard problem involving a dynamic pressure limit is discussed in [15].

It may happen that the dynamics is affine w.r.t. some of the control variables only. If we denote by u_L (resp. u_N the linear (resp. nonlinear) part of the control, sometimes Pontryagin's principle allows to express u_N as a function of (y, p) only, positively homogeneous of degree zero in p, where y (resp. p) is the state (resp. costate) variable. Substituting this expression of u_N into the dynamics of state and costate, we obtain another Hamiltonian system for a so-called *reduced Hamiltonian*. The latter is positively homogeneous of degree one in p. If the reduced Hamiltonian is affine w.r.t. u_L, then some high-order optimality conditions can be obtained, see Robbins [14].

This framework with a reduced Hamiltonian affine w.r.t. u_L applies to the launching problem, since the linear part of the control is the modulus of thrust (more exactly the ratio between the actual and maximum thrust), and the nonlinear one is the direction of thrust. The latter can be expressed as a function of the costate associated with the speed, provided that this costate is nonzero, which is the case except in pathological situations, as was discussed in [9] for academic models of launching problems. Again the singular control can be computed after two time differentiations of the switching function.

Yet several points remain to be studied. For real-world models, computing the singular control is not an easy task when some of the functions are tabulated. Also, we still do not have a theory predicting the well-posedness of the shooting equation in the case where optimal trajectories involve singular arcs (such a theory is known when the strong Legendre-Clebsch condition holds, see e.g. [3]). Actually, the latter can be set in several ways and choosing the best one is in itself a delicate task.

Another obvious difficulty with these nonconvex optimization problems is to avoid local minima. This is true for all approaches, especially for shooting algorithms [16] that have the reputation of having a small convergence radius. A classical remedy is (apart from multiple shooting, see [11, 6]) to solve an easier

problem first, and then to perform an homotopy (see for instance [1]) in order to come back to the original problem. While this procedure is often successful, it must be acknowledged that it requires some expertise. We have performed such a study and compared our results with the interior-point nonlinear programming solver IPOPT [18].

1 Problem statement

We consider here a flight mission for a heavy multi-stage launcher (Ariane 5 class). The flight takes place from the Earth to the geostationnary transfer orbit (GTO), an elliptic and slightly inclined transfer orbit used to launch satellites aimed at the geostationnary orbit (GEO). The objective is to maximize the payload of the launcher, or as a variant to minimize the fuel consumption. We will first solve the complete flight sequence to the final orbit, assuming a maximal thrust level for all propulsion systems. Then we will focus more specifically on the first atmospheric climbing phase, before the separation of the two lateral boosters, to study the existence of optimal trajectories with singular arcs.

1.1 Criterion, State and Control modelization

State variables

The state variables first include the position and speed of the launcher, both in $\mathbf{R}^3$. We also have the total mass of the launcher, which we split into the three parts of the launcher consuming fuel: m_1 for the two boosters (treated as a unique propulsion system), m_2 for the first stage, and m_3 for the second stage. This allows us to treat the separations more easily, by avoiding the discontinuities on the state variables. It should be noted that such discontinuities can be treated properly when applying Pontryagin's Minimum Principle (see for instance [12]). We actually started with this kind of approach, but the numerical experiments were disappointing, hence we tried another way around.

To finish with the masses, we also have the payload m_{CU}, which we want to maximize. This gives an additional state variable, such as $\dot{m}_{CU} = 0$ and whose initial and final values are free.

The expression of the total mass m of the launcher depends on the flight phase. The first phase lasts until the boosters separation, followed by the second phase until the first stage and hood[1] separation, and finally the third phase until the final time. Therefore the expression of the total mass is

$$\begin{array}{ll} \mathit{Phase}\ 1: & m = m_{CU} + m_1 + m_2 + m_3 + m_{hood} \\ \mathit{Phase}\ 2: & m = m_{CU} + m_2 + m_3 + m_{hood} \\ \mathit{Phase}\ 3: & m = m_{CU} + m_3 \end{array} \tag{1}$$

The original problem being with free final time, we use the standard transformation to obtain a formulation with a fixed final time

$$t = t_f.s, \quad \mathit{with}\ s \in [0,1]\ \mathit{the\ normalized\ time}. \tag{2}$$

[1]The hood is actually separated earlier in the real flight sequence, as soon as some thermal flux constraints are satisfied. We make this simplification as we do not take this kind of constraint into account here.

This brings an additional state variable t_f, which remains constant ($\dot{t}_f = 0$), and the whole dynamics is then multiplied by t_f. In the following, we will always consider the free final time formulation, unless mentioned otherwise.

Therefore the state vector is

$$x(t) = (r, v, m_1, m_2, m_3, t_f, m_{CU}) \in R^{11}. \tag{3}$$

Control variables

The control variables correspond to the thrust, and include the thrust level $\alpha \in [0, 1]$ for the boosters (we assume a maximal thrust level for the propulsion systems of the stages), and the flight angles θ and ψ (heading and azimuth) giving the thrust direction. The control vector is then

$$u = (\alpha, \theta, \psi) \in \mathbf{R} \times [-\pi, \pi]^2. \tag{4}$$

Criterion

As mentioned earlier, the objective is to maximize the payload, ie

$$Max\ m_{CU}(t_f). \tag{5}$$

Note: the payload value is constant, therefore $m_{CU}(t_f) = m_{CU}(t_0)$, the latter being part of the unknowns of the shooting problem, see below.

1.2 Flight dynamics

The dynamics for the masses correspond to the fuel consumption, which depends on the flight phase. During the first phase after the launch, both the boosters and first stage are ignited. Then boosters are separated and propulsion is from the first stage only during the second phase. After the first stage separation, the second stage is ignited for the third and last phase.

Therefore

Phase 1	*Phase* 2	*Phase* 3
$\dot{m}_1 = -\alpha\beta_{EAP}$	$\dot{m}_1 = 0$	$\dot{m}_1 = 0$
$\dot{m}_2 = -\beta_{E1}$	$\dot{m}_2 = -\beta_{E1}$	$\dot{m}_2 = 0$
$\dot{m}_3 = 0$	$\dot{m}_3 = 0$	$\dot{m}_3 = -\beta_{E2}$

(6)

where $\alpha \in [0, 1]$ is the thrust level for the boosters (part of the control) and $\beta_{EAP}, \beta_{E1}, \beta_{E2}$ are the mass flow rates for the boosters, first and second stage (we recall that the thrust level is always maximal for the latter two).

Then the flight dynamics for (r, v) are

$$\begin{cases} \dot{r} = v \\ \dot{v} = \frac{1}{m}(T(r, u) - D(r, v)) \ + \ g(r) \end{cases} \tag{7}$$

with
-$T(r, u)$: rocket thrust.

-$D(r, v)$: drag due to earth atmosphere.
-$g(r)$: gravity.

Note: we do not include here a lift term in the aerodynamic forces, according to the philosophy of a flight at null incidence. Keep in mind however that this constraint on the incidence has been removed in the present study, therefore a lift term should probably be added.

Drag force

We use the following expression for the drag force, opposite to the relative speed with respect to the air:

$$D = q\ Sr\ C_x(M) \tag{8}$$

with
- q: dynamic pressure.
- C_x: drag coefficient depending on the speed in Machs (**given by a table**).
- S_r: reference area ($S_r = 23.345m^2$).

The dynamic pressure is given by

$$q = \frac{1}{2}\gamma P_z M^2 \tag{9}$$

where
- γ: heat capacity ratio ($\gamma = 1.4$).
- P_z: atmospheric pressure at altitude z (**table**).
- M: speed in Machs, $M = V_r/V_{sound}$, V_{sound} depending on altitude (**table**).
- V_r: relative speed, $V_r = V_a - V_{air}$ with $V_a = \|v\|$ the absolute speed.

The air speed is oriented along the direction $(-\sin\ \Lambda, \cos\Lambda, 0)$ where $\Lambda = \arccos(r_1/\sqrt{r_1^2 + r_2^2})$, and its norm is:

$$V_{air} = T_{Earth}\|r\|\cos\phi \tag{10}$$

with $T_{Earth} = 7.274854\ 10^{-5}\ s^{-1}$ the rotation period of the Earth, and $\phi = \arcsin(r_3/\|r\|)$ the latitude of the launcher.

Gravity

We take the into account the J_2 correction term (earth non-sphericity) for the gravity

$$g = -\frac{\mu}{\|r\|^3}\ (r + J_2\ \frac{R_T^2}{\|r\|^2}\ M_{J_2}\ r) \tag{11}$$

with $\mu = 3.98602\ 10^{14}$, $J_2 = 0.0010826$, $R_T = 6378135$

and $M_{J_2} = \begin{pmatrix} 1 - 5\sin^2\phi & 0 & 0 \\ 0 & 1 - 5\sin^2\phi & 0 \\ 0 & 0 & 3 - 5\sin^2\phi \end{pmatrix}$.

Thrust

The general expression for a rocket thrust (in Newton) is

$$T = \alpha\beta \; Isp \; g_0 \; - S \; P_z \tag{12}$$

with
- α: thrust level in $[0, 1]$
- β: mass flow rate $(kg.s^{-1})$
- Isp: specific impulse (s)
- $g_0 = 9.81 \; m.s^{-2}$
- S: area at noozle exit (m^2)
- P_z: atmospheric pressure at altitude z

During the flight, the global thrust involves the rockets from the first and second stage (E1,E2) and the boosters (EAP). The norm of the combined thrust depends on the phase, with

$$\begin{array}{ll} Phase\ 1: & (\alpha\beta_{EAP} Isp_{EAP} + \beta_{E1} Isp_{E1}) g_0 - (S_{EAP} + S_{E1}) P_z \\ Phase\ 2: & \beta_{E1} Isp_{E1} g_0 - S_{E1} P_z \\ Phase\ 3: & \beta_{E2} Isp_{E2} g_0 \end{array} \tag{13}$$

Remark: there is no $-S \; P_z$ term for the third phase, which is already outside of the atmosphere.

along the direction

$$\begin{pmatrix} -\sin\theta \; \sin\psi \; \sin\phi \; + \; cos\theta \; cos\phi \\ \sin\theta \; \cos\psi \\ \sin\theta \; \sin\psi \; cos\phi \; + \; cos\theta \; \sin\phi \end{pmatrix} \tag{14}$$

with θ, ψ the heading and azimuth angles (part of the control in addition to the thrust level α for the boosters), and ϕ the latitude of the launcher.

1.3 Initial and final conditions

Initial conditions

The initial position of the launcher $r(0)$ is set according to the launchpad in Kourou. The initial speed $v(0)$ is also set and corresponds to the sling effect from the Earth rotation. The masses $m_1(0), m_2(0), m_3(0)$ are set according to the launcher (Ariane 5) specifications.

Therefore
- $r(0) = (6351597, 0, 581394)$
- $v(0) = (0, 462.0687, 0)$
- $m_1(0) = 556 \; 10^3$, $m_2(0) = 188 \; 10^3$, $m_3(0) = 34.2 \; 10^3$

Final conditions

First we have the final condition corresponding to the GTO orbit. In practice, this condition is not expressed directly with the Cartesian position and speed (r, v) of the launcher, but with Keplerian coordinates instead. More precisely,

we set the values of the semi-major axis, excentricity and inclination of the orbit of the launcher at t_f, namely $a_{GTO} = 2.4290635\ 10^7$, $e_{GTO} = 0.728161$ and $i_{GTO} = 0.122172$.

Note: the transformation from Cartesian to Keplerian coordinates is performed by the MSLIB *library from the CNES.*

Concerning the masses, we want here to maximize the payload m_{CU}, and we assume that all embarked fuel is consumed, with a small safety limit. Therefore we set the final conditions

$$m_i(t_f) = m_i^{empty} + m_i^{safety}, \quad i = 1, 3. \tag{15}$$

Note: the safety limit was here set to a mass corresponding to 1 second at full thrust, which is of course quite small.

2 Complete flight at full thrust

We start with solving the complete flight with stage separations, by setting a full thrust level for all propulsion systems. The next section will focus on the study of singular arcs for the boosters during the first climbing phase.

2.1 Application of Pontryagin's Minimum Principle

We detail here the application of Pontryagin's Minimum Principle to this launcher problem, and the resulting formulation for the shooting method.
We recall that we consider in this part a flight with full thrust, therefore the thrust level α is always equal to 1 for all propulsion systems (and will frequently be omitted).

Hamiltonian and costate

We introduce the costate (or *adjoint*) vector $p = (p_r, p_v, p_m, p_{t_f}, p_{m_{CU}})$, corresponding to the state variables, and assume we are in the so-called *normal case*, i.e. the adjoint asociated to the objective is non-zero, and can therefore be set to 1. This gives the expression of the Hamiltonian

$$H(x, p, u) = < p_r | v > + < p_v | \frac{T(r,u) - D(r,v)}{m} + g(r) > + < p_m | (m_1, m_2, m_3)^t > . \tag{16}$$

where m is the total mass of the launcher.

We know that any optimal pair (x, p) is solution of a Boundary Value Problem (BVP)

$$(BVP) \begin{cases} \dot{x} = \frac{\partial H}{\partial p} \\ \dot{p} = -\frac{\partial H}{\partial x} \\ \text{Boundary conditions at } t_0 \text{ and } t_f \end{cases} \tag{17}$$

where the boundary conditions include both the initial and final conditions on x and the *transversality conditions* on p (detailed below).

This Hamiltonian system gives the costate dynamics

$$\begin{cases} \dot{p}_r = -(\frac{1}{m}(T_r^t - D_r^t) + g'^t)p_v \\ \dot{p}_v = -p_r + \frac{1}{m}D_v^t p_v \\ \dot{p}_{m_i} = \frac{1}{m^2} < p_v | T - D >, \quad i = 1..3. \end{cases} \tag{18}$$

Remark: the partial derivatives of T and D involve derivating tabulated data, which is done in practice by the automatic differentiation tool TAPENADE[2].

Concerning the final time t_f, the transformation to the normalized time interval multiplies the dynamics by t_f, and therefore also the Hamiltonian. Thus derivating with respect to t_f simply gives $\dot{p}_{t_f} = -H$.

Optimal control

According to the Minimum Principle, the optimal control must minimize the Hamiltonian. The part of $H(x, p, u)$ that depends on u only comes from the thrust $T(r, u)$ (the terms form the mass dynamics do not depend on u here, as we consider full thrusts), and can be written as

$$\Phi(x, p, u) = b(x, p)\frac{< p_v | w >}{m} \tag{19}$$

where w is the normalized vector ($\in \mathbf{R}^3$) corresponding to the thrust direction given by the control angles (θ, ψ), and

$$b(x, p) = \beta_{EAP} Isp_{EAP} g_0 - S_{EAP} P_z + \beta_{E1} Isp_{E1} g_0 - S_{E1} P_z. \tag{20}$$

Note that $b(x, p)$ is actually the thrust norm and is positive.

It is known that under weak conditions p_v is nonzero, see e.g. the discussion in [9]. Therefore, minimizing $\Phi(x, p, u)$ with respect to u provides the control direction (and thus the angles (θ, ψ))

$$w = -\frac{p_v}{\|p_v\|} \tag{21}$$

Transversality conditions

Let us now detail the transversality conditions at t_0 and t_f for the costate p. At the initial time $t_0 = 0$, the values $r(0), v(0)$, $m_1(0), m_2(0)$ and $m_3(0)$ are all fixed according to the initial conditions. Therefore the corresponding costate variables $p_r(0), p_v(0)$, $p_{m_1}(0), p_{m_2}(0)$ and $p_{m_3}(0)$ are free, and will be part of the unknown of the shooting function. On the other hand, the values for $t_f(0), m_{CU}(0)$ are free, thus we have $p_{t_f}(0) = p_{m_{CU}}(0) = 0$.

[2] http://www-sop.inria.fr/tropics/tapenade.html

At the final time t_f (actually 1 for the normalized time problem), the final masses $m_i(t_f), i = 1 \dots 3$ and final time are free, therefore we have $p_i(t_f) = 0, i = 1 \dots 3$ and $p_{t_f}(t_f) = 0$. The payload $m_{CU}(t_f)$ is also free, but as our criterion is to maximize $m_{CU}(t_f)$, the transversality condition is $p_{m_{CU}}(t_f) = -1$. To finish with, we have the orbit final condition, namely $\Psi_1(r(t_f), v(t_f)) = 0$, with

$$\begin{array}{rl} \Psi_1 : & \mathbf{R}^6 \to \mathbf{R}^3 \\ & (r, v) \mapsto (a, e, i) - (a_{GTO}, e_{GTO}, i_{GTO}) \end{array} \tag{22}$$

where a, e, i are the Keplerian parameters: semi-major axis, eccentricity and inclination of the orbit, that can be computed from the Cartesian position and speed. Thus there exists $\mu_1 \in \mathbf{R}^3$ such that

$$p_r(t_f) = \frac{\partial \Psi_1}{\partial r}^t \mu_1, \quad \textit{and } p_v(t_f) = \frac{\partial \Psi_1}{\partial v}^t \mu_1. \tag{23}$$

This change of coordinates is such that the derivative of Ψ is surjective, so that μ can be eliminated from these equations. For our problem $\frac{\partial \Psi_1}{\partial r}^t$ is invertible, and so we can write the transversality condition as

$$p_v(t_f) - \frac{\partial \Psi_1}{\partial v}^t \left(\frac{\partial \Psi_1}{\partial r}^t\right)^{-1} p_r(t_f) = 0. \tag{24}$$

Separation times

As we model the mass of each component of the launcher separately, the separation times do not introduce discontinuities of the state variables, even if the total mass of the launcher is discontinuous at these times. Therefore the separation times t_1 and t_2 for the boosters and first stage only need to satisfy the continuity of the Hamiltonian.

As this condition is numerically quite hard to satisfy properly, we introduce as additional shooting unknowns the value of the state and costate at the separation times, namely (x^1, p^1) and (x^2, p^2). Then we have the corresponding matching conditions with the integrated state and costate at t_1 and t_2, which are just the continuity of x and p.

Remark: it is possible to reduce the number of state variables by taking the total mass as a state variable. Then the state is discontinuous at time of separation. The corresponding shooting system can be obtained, see for instance [12]. However, this formulation did not give good numerical results in our case, and hence we chose to split the total mass into three state variables to get rid of the discontinuities.

Shooting problem formulation

We summarize here the formulation of the shooting problem for the complete flight with maximal thrust.

• **Shooting function unknown $z \in \mathbf{R}^{57}$:**

$$z = (t_f, m_{CU}, p_r(0), p_v(0), p_m(0), x^1, p^1, x^2, p^2, t_1, t_2).$$

• **Shooting function value** $S(z) \in \mathbf{R}^{57}$**:**

$$\begin{cases} (a(t_f), e(t_f), i(t_f)) - (a_{GTO}, e_{GTO}, i_{GTO}) & \textit{Final orbit condition} \\ p_v(t_f) - \frac{\partial \Psi_1}{\partial v}^t (\frac{\partial \Psi_1}{\partial r}^t)^{-1} p_r(t_f) & \textit{Final orbit TC} \\ p_{t_f}(t_f) & \textit{Final time TC} \\ m_i(t_f) - (m_i^{empty} + m_i^{safety}) \quad , i = 1..3 & \textit{Final masses condition} \\ p_{m_{CU}} + 1 & \textit{Payload maximization TC} \\ H|t_i^+ - H|t_i^- \quad , i = 1..2 & \textit{Hamiltonian continuity} \\ (x(t_i), p(t_i)) - (x^i, p^i) \quad , i = 1, 2 & \textit{Matching conditions} \end{cases} \tag{25}$$

2.2 Numerical results

Solving the complete flight problem directly with the shooting method is difficult, due to the lack of a suitable initial guess. However, restricting the flight to the first phase (until separation of the boosters) gives a much easier problem that we are able to solve from a simple starting point. This solution is sufficient to solve the problem if we add the second phase of the flight (until separation of the first stage). Then we finally solve the complete flight from this second solution. We find a solution with a payload of 14623kg and a final time of 1232.75 seconds. The separation of the boosters occurs after 119 seconds, and 533.375 seconds for the stage, which is consistent with the constraints set on the final masses (consumption of all fuel).

Remark: the thrust is actually completely fixed during the first 10 seconds of the flight, vertical and maximal.

The first two graphs represent the optimal control (with the thrust level for the boosters and two stages, here set to 1, and the heading and azimuth angles for the thrust direction), and the masses of the different parts of the launcher. The separations correspond to the discontinuities observed on the total mass.

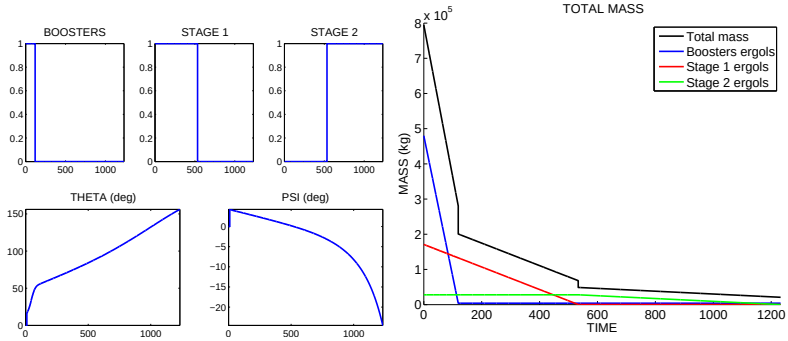

Complete flight with full thrust - Controls and masses

We show now the evolution of the altitude and speed of the launcher during the flight. The change of propulsion system at the beginning of the second and third phases is clearly visible on the speed graph. These graphs are consistent

with the typical GTO flight described for instance in the Ariane 5 User's Manual (Issue 4) from Arianespace.

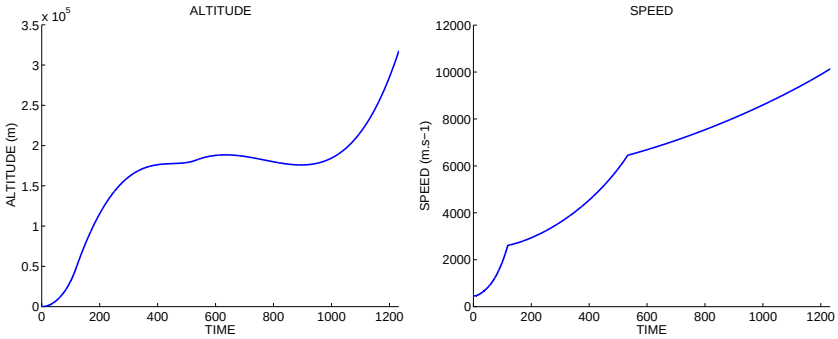

Complete flight with full thrust - Altitude and speed

To finish with, we draw the trajectory of the launcher around the Earth, with its projection on the equatorial plane.

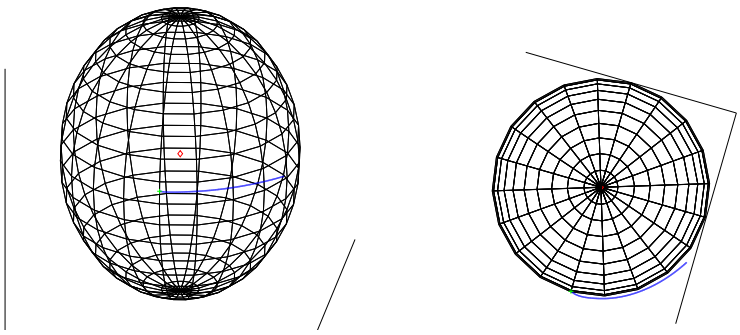

Complete flight with full thrust - Trajectory

Remark: It should be kept in mind that we have allowed a free direction for the thrust, which is not the case in the real flight, where the thrust is along the launcher axis almost all the time.

3 Study of singular arcs for the first phase

We focus now on the study of singular arcs for the thrust level of the boosters, which is now free in $[0, 1]$, while we keep a maximal thrust level (equal to 1) for the two stages.

3.1 Application of the Minimum Principle

We detail here again the application of Pontryagin's Minimum Principle, but this time taking into account the possible existence of singular arcs.

New modelization

We now restrict the flight to the first atmospheric climbing phase, until the separation of the boosters. This allows us to reformulate the payload maximization criterion into a fuel consumption minimization, more suitable for the study of singular arcs. There are no stage separations anymore, and maximizing the payload is the same as maximizing the final mass of the launcher, which is equivalent to minimizing the fuel consumption. As we consider a variable thrust level for the boosters only, we set as the new criterion

$$Min \int_0^{t_f} \alpha \ \beta_{EAP}. \tag{26}$$

Concerning the masses, the payload is now fixed and is no longer part of the state variables, and the final masses m_1, m_2, m_3 are free.

We also replace the final condition on the orbit by new final conditions on the position and speed. We take the values corresponding to the boosters separation on the trajectory found previously for the complete flight with full thrust, and set

$$\begin{array}{ll} r_f & = (6397703.2500, 108068.5570, 582834.1620) \\ v_f & = (934.2087, 2088.7070, 84.8210) \end{array} \tag{27}$$

New criterion and Hamiltonian

Compared to the full thrust problem, now $\alpha \in [0, 1]$ and is not set to 1 anymore, and we have an additional term in the Hamiltonian corresponding to the new criterion, therefore

$$H(x, p, u) = \alpha\beta_{EAP} + < p_r | v > + < p_v | \frac{T(r, u) - D(r, v)}{m} + g(r) > + \sum_{i=1}^{3} p_i \dot{m}_i \tag{28}$$

As the derivatives of the $\alpha\beta_{EAP}$ term with respect to the state x are zero, the dynamics of the costate p are the same as before.

Optimal control

So the optimal control $(\alpha, w) \in [0, 1] \times S_3(0, 1)$ must minimize

$$\Phi(x, p, u) = a(x, p)\alpha + b(x, p, \alpha)\frac{< p_v | w >}{m} \tag{29}$$

with $a(x, p) = (1 - p_{m_1})\beta_{EAP}$
and $b(x, p, \alpha) = \|T\| = \alpha \ \beta_{EAP} Isp_{EAP} g_0 - S_{EAP} P_z + \beta_{E1} Isp_{E1} g_0 - S_{E1} P_z$.

As α and w are independent (and the thrust norm $b(x, p, \alpha)$ is positive), we still have $w = -\frac{p_v}{\|p_v\|}$. Replacing w by this value in Φ, the thrust level α must minimize the expression

$$(a(x, p) - \beta_{EAP} Isp_{EAP} g_0 \frac{\|p_v\|}{m})\alpha. \tag{30}$$

We define the **switching function**

$$\psi(x,p) = a(x,p) - \beta_{EAP} Isp_{EAP} g_0 \frac{\|p_v\|}{m}, \tag{31}$$

and have the following command law

$$\begin{cases} If \quad \psi(x,p) > 0 \quad then \quad \alpha = 0 \\ If \quad \psi(x,p) < 0 \quad then \quad \alpha = 1 \\ If \quad \psi(x,p) = 0 \quad then \quad \alpha \in [0,1] \rightarrow \text{switching point or singular arc.} \end{cases} \tag{32}$$

Singular arcs

In case of a singular arc, i.e. a time interval over which the switching function ψ vanishes, the thrust level α may belong to $(0,1)$. According to [8, 14, 4], the value of the singular control can be obtained from the successive time derivatives of the switching function, that must all vanish. For instance, in the case of the 3D Goddard problem we studied in [9], the formal expression of α_{sing} is given by solving the equation $\ddot{\psi} = 0$, which was done in practice with the symbolic calculus tool MAPLE[3]. We shall see below that in the present case, this method had to be adapted due to the presence of tabulated data in the thrust and drag terms.

The shooting formulation can be adapted to the case of singular arcs as follows. The structure of the control must be prescribed by assigning a fixed number of interior switching times that correspond to junctions between non-singular and singular arcs. Depending on the nature of the current arc, the integration of (IVP) uses either the control given by the Hamiltonian minimization above, or the singular control obtained by the method presented below. These times $(t_i)_{i=1..n_{switch}}$ are part of the unknowns and must satisfy some switching conditions. Considering that the singular control is often computed using the relation $\ddot{\psi} = 0$, switching conditions may consist for instance in requiring either $\psi = 0$ at both extremities of the singular arc, or $\psi = \dot{\psi} = 0$ at the beginning of the arc. In our simulations, we choose the latter solution which happens to provide better and more stable results.

Transversality conditions

As the initial conditions are unchanged, the transversality conditions at the initial time are the same as for the complete flight.

At the final time, the orbit condition is replaced with the simpler condition on $r(t_f), v(t_f)$, thus $p_r(t_f)$ and $p_v(t_f)$ are free. Also, the final masses m_1, m_2, m_3 being now free, we have the corresponding transversality conditions $p_m(t_f) = 0$.

Shooting formulation

Here is the formulation of the shooting problem for a solution with one interior singular arc.

[3] http://www.maplesoft.com

• **Shooting function unknown** $z \in \mathbf{R}^{12}$**:**

$$z = (t_f, p_r(0), p_v(0), p_m(0), t_1, t_2).$$

• **Shooting function value** $S(z) \in \mathbf{R}^{12}$**:**

$$\left\{ \begin{array}{ll} r(t_f) - r_f & \textit{Final position} \\ v(t_f) - v_f & \textit{Final speed} \\ p_{t_f}(t_f) & \textit{Final time TC} \\ p_i(t_f)\ , i = 1..3 & \textit{Final masses TC} \\ \psi(x(t_1), p(t_1)) & \textit{Switching conditions} \\ \dot{\psi}(x(t_1), p(t_1)) & \end{array} \right. \tag{33}$$

Remark: concerning the switching times for the singular arcs, it is also possible to include in the shooting unknown the value of the state and costate at these times, which must then satisfy some matching conditions (namely the continuity of x, p *in this case, same as for the separation times in the previous study of the complete flight).*

3.2 An alternate expression for the singular control

As mentioned above, the expression of the singular control for the level thrust α is theoretically obtained from the second derivative of the switching function, namely the equation $\ddot{\psi}(x,p) = 0$. However, in this case the analytic expression of $\ddot{\psi}$ is not available, due to the presence of tabulated data in the thrust and drag terms. The first derivative $\dot{\psi}$, on the other hand, only involves $\dot{x}$ and $\dot{p}$, so we have its analytic expression from the state-costate dynamics. As the idea behind the formal expression of the singular control is that the switching function[4] and its successive derivatives with respect to time vanish over a singular arc, we try here to enforce this constraint with the terms at our disposal.

Therefore, we choose for the singular control the value $\tilde{\alpha}_{sing}$ that minimizes ψ and $\dot{\psi}$ at the next integration step, ie

$$\tilde{\alpha}_{sing} = ArgMin_{[0,1]}\ \|(\psi(y_{i+1}), \dot{\psi}(y_{i+1}))^t\|^2 \ = \ \psi^2(y_{i+1}) + \dot{\psi}^2(y_{i+1}), \tag{34}$$

where y_{i+1} denotes the state-costate pair (x,p) obtained after one integration step from the current time. This minimization in dimension one is currently performed by a BFGS method [5], starting from an initial value $\alpha = 0.5$. While for one dimensional problems the BFGS algorithm is in fact a (safeguarded) secant method, it was convenient to use a quasi-Newton code. The numerical experiments showed that taking 0.1 or 0.9 as initial values gives similar results, which is of course reassuring.

Testing this formulation on the generalized Goddard problem (cf [9]) indicates that we find control values quite close to the exact value α^*_{sing} obtained from the equation $\ddot{\psi}(x,p) = 0$ (except the value at the entry point on the singular arc).

[4] or more generally, the derivative of the Hamiltonian with respect to the control

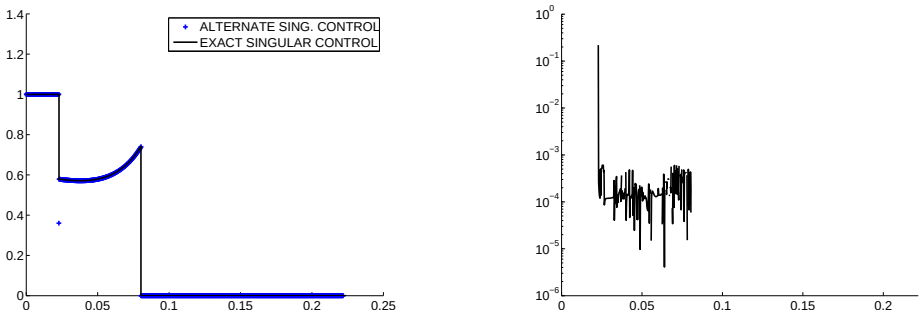

Approximate and exact singular control - $Log_{10}|\alpha^*_{sing} - \tilde{\alpha}_{sing}|$

So this alternate formulation seems to give satisfactory results on the simplified launcher problem. It should be noticed that the computational cost is significantly increased, however the minimization procedure was not optimized and might be further improved.

3.3 Continuation approach for singular arcs

In order to solve a problem with singular arcs, besides the expression of the singular control, we also need some information about the control structure, namely the number and position of the singular arcs. The approach we use to obtain such information is to approach the original problem by a sequence of regualarized problems with strictly convex Hamiltonians (with respect to the control), such as in [10, 9] for instance. This is done by adding a quadratic term to the criterion, which becomes, for given $\lambda \in [0, 1]$:

$$Min \int_0^{t_f} \left[\alpha\ \beta_{EAP} + (1-\lambda)\ \alpha^2 \beta_{EAP}\right] \mathrm{d}t. \tag{35}$$

We obtain a family of regularized problems $(P)_\lambda$ such that $(P)_1 = (P)$ the original, unperturbed problem. This regularization adds a new term $(1-\lambda)\ \alpha^2\beta_{EAP}$ to the Hamiltonian, which gives the modified command law for $\lambda < 1$:

$$\left\{\begin{array}{lll} If & \psi(x,p) > 0 & then \quad \alpha = 0 \\ If & \psi(x,p) < -2(1-\lambda)\beta_{EAP} & then \quad \alpha = 1 \\ If & -2(1-\lambda)\beta_{EAP} < \psi(x,p) < 0 & then \quad \alpha = \frac{-\psi(x,p)}{2(1-\lambda)\beta_{EAP}}. \end{array}\right. \tag{36}$$

As we can see, there are no singular arcs anymore. Moreover, since the Hamiltonian is strictly convex with respect to the control, the optimal control is actually continuous (no switchings).

We perform a discrete continuation on this problem family, and try to solve a sequence of problems $(P)_\lambda$, starting from $\lambda = 0$ to $\lambda = 1$. Notice that we do not actually try to reach $\lambda = 1$, since we would encounter difficulties if singular arcs are present. We only need to reach a value of λ close enough to 1 so that we gain sufficient information regarding the control structure. Moreover, we want to use the corresponding solution to initialize the shooting method adapted to cas of the singular arcs.

However, it happens that even the strongly regularized problem $(P)_0$ is not easy to solve directly with the shooting method. This is why we add a first phase consisting in a homotopy over atmospheric forces, gradually introducing the atmospheric drag for the problem $(P)_0$. We will see that the regularized problem without drag is usually easy to solve, and that the continuation on the drag is also easy to complete, which gives a solution for the regularized problem $(P)_0$. We can then begin the regularization homotopy in order to determine the control structure. The results of this method are described below, first for the original launcher, and then for a slightly modified launcher.

3.4 Study of the original launcher

We first apply the approach described above to the original launcher problem, with a fixed payload $m_{CU} = 12610kg$. The regularized problem without any drag forces can be solved from a very simple starting point ($t_f = 100$, $p_r(0) = (-0.1, -0.1, 0.1)$, $p_v(0) = (-10^3, -10^3, -10^3)$ and $p_i(0) = -0.1, i = 1 \dots 3$). The preliminary continuation is performed without any difficulties and gives a solution of $(P)_0$. The regularization homotopy is then able to reach until $\lambda = 0.999$, however the results are rather disappointing concerning the singular structure of the control. The following graph shows the evolution of the thrust level for the boosters during the continuation, for values of the homotopic parameter λ ranging from 0 to 0.999.

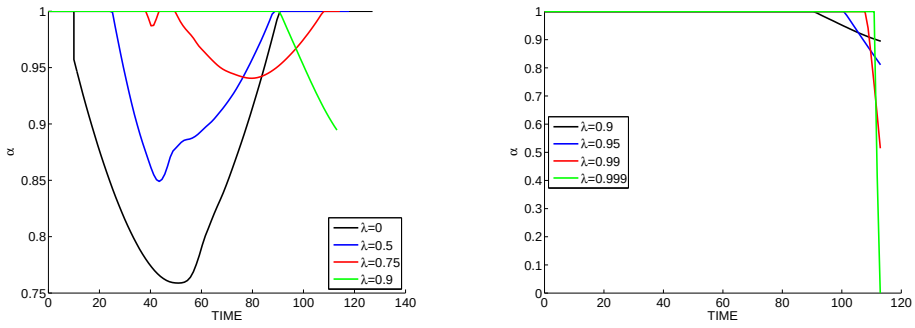

Regularization homotopy: thrust level for $\lambda = 0, 0.5, 0.75, 0.9, 0.95, 0.99, 0.999$

We observe that the interval with a non-maximal thrust becomes smaller when the regularization decreases as λ tends to 1. At $\lambda = 0.999$, we have a solution with a full thrust during all the flight except for the last few seconds, and no sign of a singular arc. Simple experiments with a direct method (piecewise constant control with 100 steps, Runge Kutta 4 integration for the state, IPOPT solver for the resulting optimization problem) give a similar solution, with a full thrust and a switching to null thrust just before the end of the flight. The fact that both methods seem to indicate the absence of time intervals with a non-maximal (and non-zero) thrust strongly suggests that the optimal solution for this problem does not present singular arcs.

3.5 Study of a modified launcher

Now we try to modify the launcher parameters in order to obtain an optimal solution with singular arcs. More precisely, we want to increase the atmospheric

drag and the thrust of the launcher. A simple way to do this is to increase the reference area S_r and the specific impulsion Isp_{EAP}. We show here the results corresponding to $S_r \times 2$ and $Isp_{EAP} \times 1.25$.

As before, the regularized problem with no drag is easily solved, and the first continuation to introduce the drag poses no difficulties. Then we perform the regularization continuation until $\lambda = 0.95$, and this time find strong hints of a singular arc. The following graphs show the thrust level and switching function at the solutions for $\lambda = 0$, 0.5, 0.9 and 0.95. Contrary to the previous case, we observe a small time interval (around $t = 30s$) where the thrust level remains in $]0, 1[$. Moreover, we see that the switching function ψ comes closer to 0 on the same time interval. These two facts together strongly suggest the presence of a singular arc. What happens at the end of the flight is less clear, as the thrust level takes again values in $]0, 1[$, and decreases near t_f. This could indicate a second singular arc, maybe followed by an arc with a null thrust, or just a switching to a null thrust arc.

Remark: we recall that the thrust is fixed during the first 10 seconds of the flight, vertical and maximal. We arbitrarily set the switching function to 0 during this time.

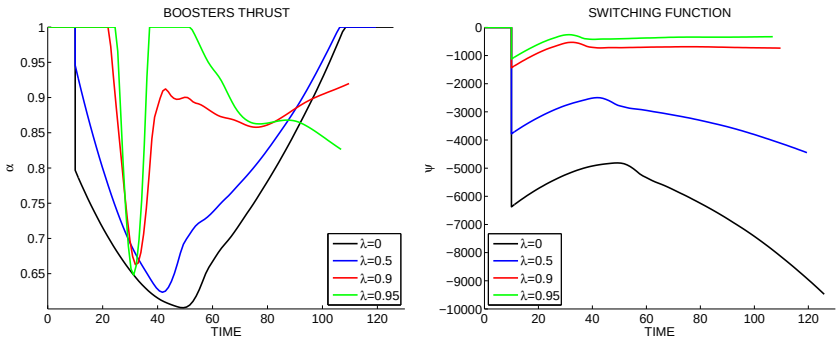

Regularization homotopy: thrust level and switching function for $\lambda = 0, 0.5, 0.9, 0.95$

We try to apply the shooting method for the three control structures:
- **bang - sing - bang**
- **bang - sing - bang - sing**
- **bang - sing - bang - sing - bang**

For both structures with two singular arcs the shooting method fails to converge, while the first formulation actually gives a solution with a singular arc and a switching at the end. We check that the solutions obtained with the regularization homotopy seem to converge to this solution with a singular arc. Once again, we test a basic direct method, and find a similar solution.

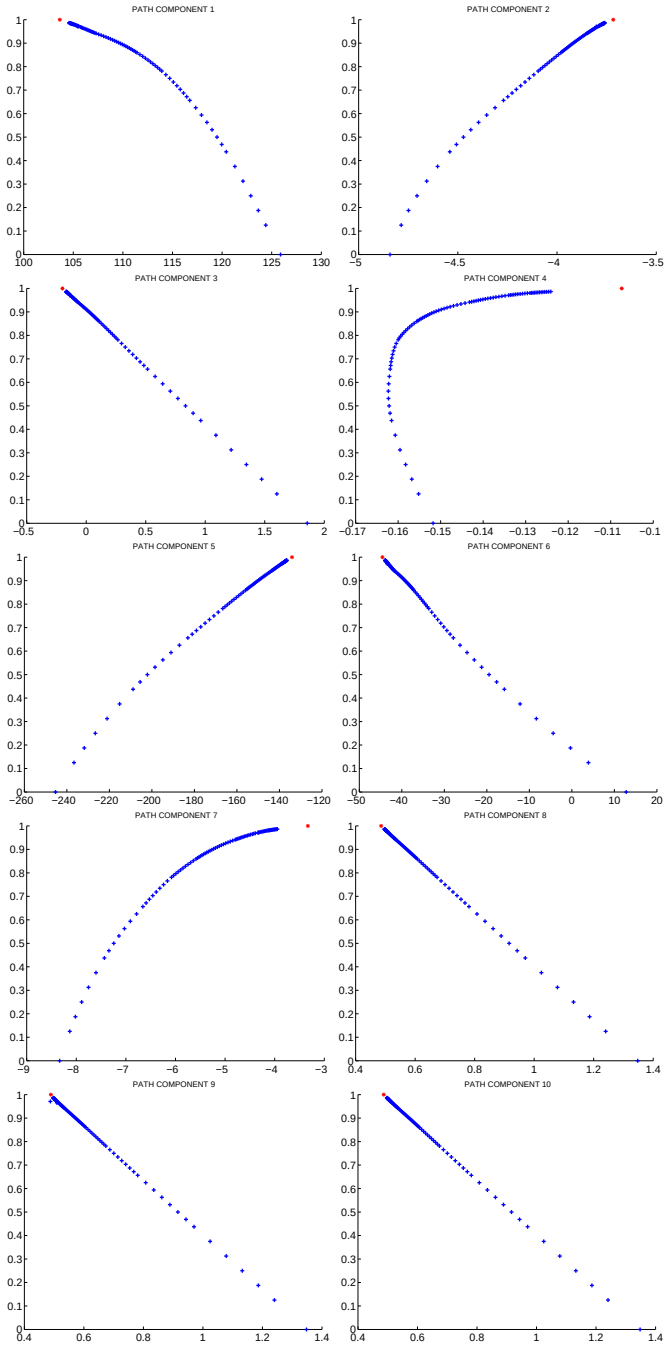

Regularization homotopy and solution with singular arc

The following graph shows the thrust level, the small singular arc (about 3 seconds) being clearly visible on both solutions from the indirect and direct methods, around $t = 30s$. Both solutions also confirm that we have a simple switching near the end of the flight, and not a second singular arc.

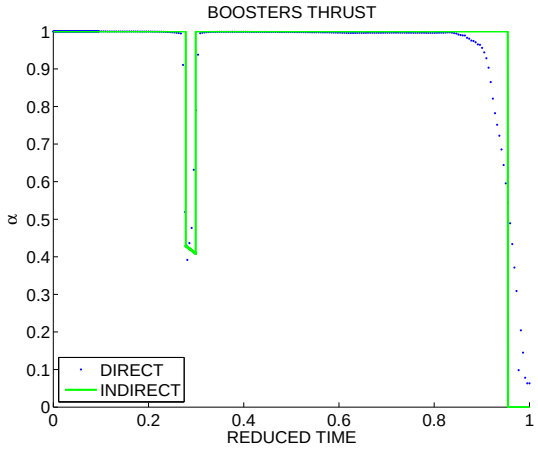

Solution with singular arc - structure: bang(1) - sing - bang(1-0)

We draw now the heading and azimuth angles, corresponding to the thrust direction. We see that both solutions are quite close, except at the end of the flight near the switching, where the solution from the direct method is less accurate (keep in mind, however, that we used a very rough formulation for our experiments with the direct method, as we only wanted to check the solution from the shooting method; it is probably possible to obtain a much cleaner solution with a more elaborate direct method).

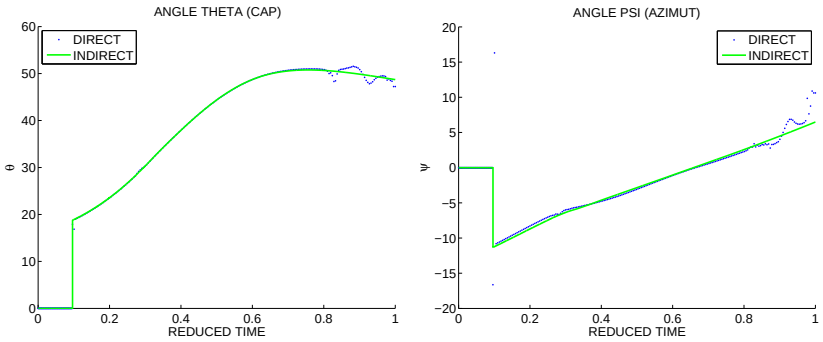

Heading and azimuth angles (thrust direction)

To finish with, we have a look at the switching function ψ and its first derivative $\dot{\psi}$. As expected, both are close to 0 on the singular arc (recall that the value for the first ten seconds is arbitrary as the control is fixed), and we see the sign change corresponding to the switching at the end of the flight. The second graph is a close-up on the singular arc, and shows that the approach of computing the singular control that minimizes $\psi^2 + \dot{\psi}^2$ works rather well, with a range of 10^{-3} for ψ and 10^{-4} for $\dot{\psi}$.

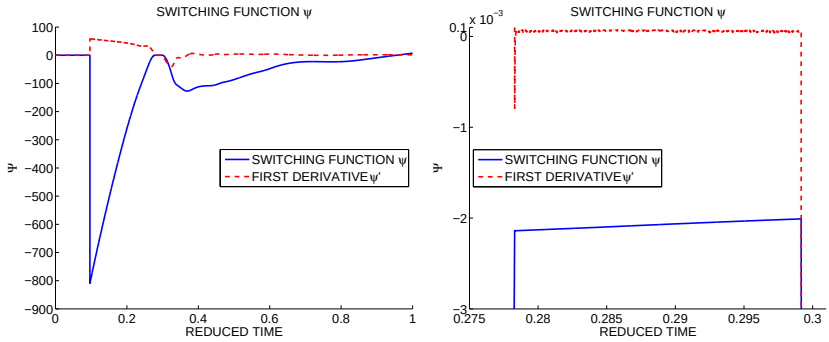

Solution with singular arc - switching function ψ, and $\dot{\psi}$

The criterion value (i.e. final mass of the EAP) is quite close for both solutions, with $m_1(t_f) = 165163kg$ for the shooting method and $m_1(t_f) = 164990kg$ for the direct method. Incidentally, solving the same problem with the direct method when forcing a bang(1)-bang(0) control structure gives a close solution (without the singular arc of course), with a criterion of $m_1(t_f) = 164442kg$. It is comforting to observe that the solution with the singular arc is indeed slightly better than the forced bang-bang one, even if the difference is quite small. It seems reasonnable to assume that for a different set of parameters that would give a solution with a longer singular arc, the gain compared to the bang-bang solution would be more significant. Indeed, we can perform a continuation directly on the solution with a singular arc, and further increase the value of the parameter S_r. We observe that the solutions exhibit longer singular arcs when S_r increases, with a more important gain with respect to the corresponding solution.

	$S_r \times 2$	$S_r \times 2.5$	$S_r \times 3$
$m_1(t_f)$ (singular arc)	165163 kg	160199 kg	155986 kg
$m_1(t_f)$ (bang-bang)	164442 kg	159172 kg	154202 kg
Mass gain	721 kg	1027 kg	1784 kg

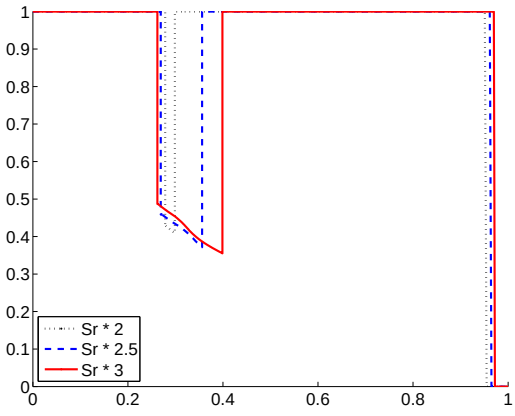

Singular arcs for increasing values of S_r

Remark: it is also possible to perform a continuation on the parameters Isp_{EAP} and β_{EAP}, for instance, that show that increasing these values also leads to longer singular arcs. However, these continuations are numerically more

difficult than restarting from the atmosphere and regularization homotopies, and allow only a small modification of the parameters.

Conclusion

We focus in this study on the practical computation of optimal trajectories for a space launcher problem in presence of singular arcs. The main idea is to use a continuation approach with the shooting method, with a quadratic regularization of the objective function to approximate the singular structure of the control. This method was successfully applied to the generalized (3D) Goddard problem (see [9]) and is here extended to the case where the analytic expression of the singular control is not available. Our experiments indicate that while the original problem for an Ariane 5 launcher seems to admit a bang-bang optimal solution, slightly modifying some parameters such as the reference aera and specific impulsion of the launcher gives an optimal solution with a singular arc. Future perspectives in the following of this work include the study of launcher models with wings (subject to a lift force), and taking into account a mechanical structure constraint (limiting the angle between the thrust and launcher axis).

Note: all numerical simulations were run on a standard desktop computer (Pentium IV 2.4GHz), using the gfortran [5] *fortran compiler.*

References

[1] E. Allgower and K. Georg. *Numerical Continuation Methods*. Springer-Verlag, Berlin, 1990.

[2] J.T. Betts. Survey of numerical methods for trajectory optimization. *AIAA J. of Guidance, Control and Dynamics*, 21:193–207, 1998.

[3] J.F. Bonnans and A. Hermant. Well-posedness of the shooting algorithm for state constrained optimal control problems with a single constraint and control. *SIAM J. Control Optimization*, 46(4):1398–1430, 2007.

[4] A. E. Bryson and Y.-C. Ho. *Applied optimal control*. Hemisphere Publishing, New-York, 1975.

[5] R.H. Byrd, P. Lu, J. Nocedal, and C.Y. Zhu. A limited memory algorithm for bound constrained optimization. *SIAM J. Sci. Comput.*, 16(5):1190–1208, 1995.

[6] H.-J. Diekhoff, P. Lory, H.J. Oberle, H.-J. Pesch, P. Rentrop, and R. Seydel. Comparing routines for the numerical solution of initial value problems of ordinary differential equations in multiple shooting. *Numerische Mathematik*, 27:449–469, 1977.

[7] R.H. Goddard. *A Method of Reaching Extreme Altitudes*, volume 71(2) of *Smithsonian Miscellaneous Collections*. Smithsonian institution, City of Washington, 1919.

[5] http://gcc.gnu.org/fortran/

[8] B.S. Goh. Necessary conditions for singular extremals involving multiple control variables. *J. SIAM Control*, 4:716–731, 1966.

[9] P. Martinon, J.F. Bonnans, and E. Trélat. Singular arcs in the generalized Goddard's problem. *J. Optimization Theory Applications*, 138, 2008. To appear. Preprint: INRIA Report RR-6157.

[10] P. Martinon and J. Gergaud. An application of PL continuation methods to singular arcs problems. In *Recent advances in optimization*, volume 563 of *Lecture Notes in Econom. and Math. Systems*, pages 163–186. Springer, Berlin, 2006.

[11] H. Maurer. Numerical solution of singular control problems using multiple shooting techniques. *J. of Optimization Theory and Applications*, 18:235–257, 1976.

[12] H. J. Pesch. A practical guide to the solution of real-life optimal control problems. *Control and Cybernetics*, 23:7–60, 1994.

[13] H.J. Pesch. Real-time computation of feedback controls for constrained optimal control problems II: a correction method based on multiple shooting. *Optimal Control, Applications and Methods*, 10:147–171, 1989.

[14] H.M. Robbins. A generalized Legendre-Clebsch condition for the singular case of optimal control. *IBM J. of Research and Development*, 11:361–372, 1967.

[15] H. Seywald and E.M. Cliff. Goddard problem in presence of a dynamic pressure limit. *Journal of Guidance, Control, and Dynamics*, 16(4):776–781, 1993.

[16] J. Stoer and R. Bulirsch. *Introduction to Numerical Analysis*. Springer-Verlag, New-York, 1993.

[17] P. Tsiotras and H.J. Kelley. Drag-law effects in the Goddard problem. *Automatica*, 27-3:481–490, 1991.

[18] A. Waechter and L.T. Biegler. On the implementation of an interior-point filter line-search algorithm for large-scale nonlinear programming. *Mathematical Programming Series A*, 106:25–57, 2006.

Centre de recherche INRIA Saclay – Île-de-France
Parc Orsay Université - ZAC des Vignes
4, rue Jacques Monod - 91893 Orsay Cedex (France)

Centre de recherche INRIA Bordeaux – Sud Ouest : Domaine Universitaire - 351, cours de la Libération - 33405 Talence Cedex
Centre de recherche INRIA Grenoble – Rhône-Alpes : 655, avenue de l'Europe - 38334 Montbonnot Saint-Ismier
Centre de recherche INRIA Lille – Nord Europe : Parc Scientifique de la Haute Borne - 40, avenue Halley - 59650 Villeneuve d'Ascq
Centre de recherche INRIA Nancy – Grand Est : LORIA, Technopôle de Nancy-Brabois - Campus scientifique
615, rue du Jardin Botanique - BP 101 - 54602 Villers-lès-Nancy Cedex
Centre de recherche INRIA Paris – Rocquencourt : Domaine de Voluceau - Rocquencourt - BP 105 - 78153 Le Chesnay Cedex
Centre de recherche INRIA Rennes – Bretagne Atlantique : IRISA, Campus universitaire de Beaulieu - 35042 Rennes Cedex
Centre de recherche INRIA Sophia Antipolis – Méditerranée : 2004, route des Lucioles - BP 93 - 06902 Sophia Antipolis Cedex

Éditeur
INRIA - Domaine de Voluceau - Rocquencourt, BP 105 - 78153 Le Chesnay Cedex (France)
http://www.inria.fr
ISSN 0249-6399